Available online at www.sciencedirect.com
SCIENCE DIRECT®
Journal of Sound and Vibration 289 (2006) 1–24
JOURNAL OF SOUND AND VIBRATION
www.elsevier.com/locate/jsvi

Free vibration analysis by the superposition method of rectangular Mindlin plates with internal columns resting on uniform elastic edge supports

Fumito Ohya[a,*], Masaiki Ueda[a], Takeshi Uchiyama[b], Masaru Kikuchi[a]

[a]*Graduate School of Engineering, Hokkaido University, Kita 13, Nishi 8, Kita-ku, Sapporo, Hokkaido 060-8628, Japan*
[b]*Faculty of Fine Arts, Dohto University, 149 Nakanosawa, Kitahiroshima, Hokkaido 061-1196, Japan*

Received 17 June 2004; received in revised form 7 January 2005; accepted 28 January 2005
Available online 12 April 2005

Abstract

Free vibration analysis of rectangular Mindlin plates is carried out via the superposition method and is shown to produce accurate results. The analytical method proposed by the authors in this paper solves the problem for the case where the plate has simultaneous elastic edge and internal supports. The conditions of edge supports are uniform lateral, rotational and torsional elastic supports, whereas, the internal supports are column supports with finite area. Compatibility between the plate and column is achieved by requiring that the column and plate rotations be equal. The results presented herein are verified through comparison with results presented by others. Numerical examples presented in this study confirm that the analytical method is able to model the property of the elastic edge supports while simultaneously considering the effect of column restraint, an effect which increases with column number and area.

1. Introduction

The modeling of rectangular plates with inner and edge supports is important in many branches of engineering. The applications include the modeling of slabs supported by columns, printed circuit boards and panels in ships and aircrafts. With its potential applications, the vibration of

*Corresponding author. Tel./fax: +81 11 706 5333.
E-mail address: ohyashi@eng.hokudai.ac.jp (F. Ohya).

0022-460X/$ - see front matter © 2005 Elsevier Ltd. All rights reserved.
doi:10.1016/j.jsv.2005.01.030

Nomenclature

$2a, 2b$	lengths of rectangular plate edge in the x and y directions
a', b'	span lengths in the x and y directions
c', d'	cantilever lengths in the x and y directions
l	column length
$2u, 2v$	widths of the column section in the x and y directions
h	plate thickness
ϕ	plate aspect ratio
w	plate lateral displacement
ψ_x, ψ_y	plate cross-section rotations associated with x and y directions
ω	radian natural frequency
λ	$= \omega a^2\sqrt{\rho h/D}$, frequency parameter
D	flexural rigidity of the plate
G	shear modulus
E	Young's modulus
I	second moment of area in the column
A	column area
ρ	density
v	Poisson ratio
κ	shear correction factor
K_L	lateral stiffness of elastic edge support
K_R	rotational stiffness of elastic edge support
K_T	torsional stiffness of elastic edge support
μ_m, μ_n	$= m\pi, = n\pi$ (for the SS Mode only. See Eq. (7) for other mode.)
N	total number of columns
${}_c\Psi_x$, ${}_c\Psi_y$	rotations of the column associated with x and y directions
${}_s\Psi_x$, ${}_s\Psi_y$	rotations of the plate associated with x and y directions
${}_iM_x$, ${}_iM_y$	bending moments of the ith column associated with x and y directions
${}_tP$	total vertical force over all columns
${}_iP$	partial vertical force on the ith column
${}_tM_x$, ${}_tM_y$	total bending moments over all columns associated with x and y directions
${}_iM_x$, ${}_iM_y$	bending moments at the ith column associated with x and y directions

plates with inner supports and elastically restrained edges has received considerable attention from researchers.

It is well known that the edge boundary conditions greatly influence the free vibration characteristics of rectangular plates. The classical edge conditions (clamped, free or simply supported) are relatively easy to formulate, however, difficult to apply in practice. Therefore, considerable research has been devoted to the free vibration analysis of plates resting on elastic edge supports. Gorman [1,2] studied the free vibration of rectangular plates with elastic edge supports based on the thin plate theory and the Mindlin plate theory using the superposition method. Xiang et al. [3] used polynomials and basic functions as the admissible functions to analyze the vibration of rectangular Mindlin plates with elastic edge supports by the Ritz method. Saha et al. [4] used the vibrating Timoshenko beam functions, and Zhou [5] applied the static Timoshenko beam functions, as the admissible function to investigate the same problem by the Rayleigh–Ritz method. Free vibration analysis of rectangular plates with inner supports has also been considered by many researchers. Gorman [6,7] presented the solutions for rectangular plates with point supports, based on the thin plate theory and the Mindlin plate theory by the superposition method. Liew et al. [8] investigated Mindlin plates of arbitrary shapes with internal point supports by the Rayleigh–Ritz method. Huang and Thambiratnam [9] studied rectangular plates on elastic intermediate supports using the finite strip element method combined with a spring system.

The above publications have focused on the case of either elastic edge supports or inner supports alone, and there is little or no reported research for the free vibration analysis of Mindlin

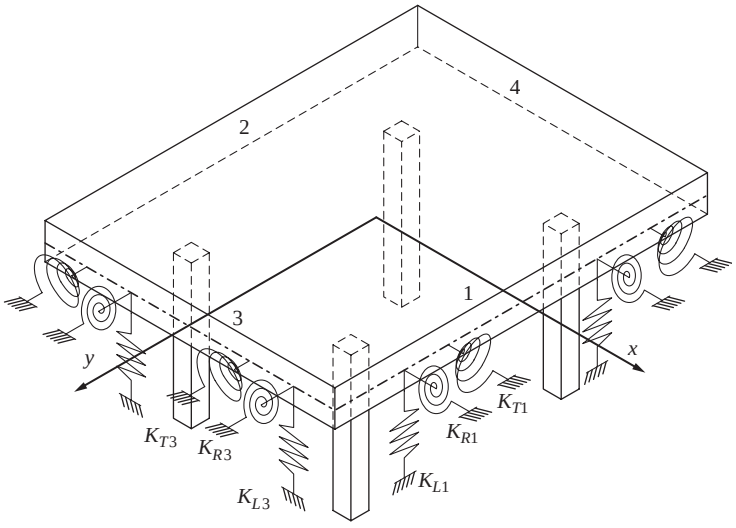

Fig. 1. Schematic of rectangular Mindlin plate with internal columns; the uniform elastic edge supports are represented by lateral (K_L), rotational (K_R) and torsional (K_T) springs.

plates with simultaneous elastic edge and internal supports. Therefore, the purpose of this paper is to propose an analytical method for dealing with these simultaneous support conditions. This analytical method makes possible the free vibration analysis of rectangular plates with elastic edge supports and with internal column supports by the superposition method based on Mindlin plate theory. The classical thin plate theory results in errors which increase as the ratio of the plate thickness to span ratio increases, so in this study, the Mindlin plate theory is employed which considers the effect of transverse shear deformation and rotary inertia. The boundary conditions of elastic edge supports are uniform lateral, rotational and torsional elastic supports. The internal supports are column supports with finite area. Compatibility between the plate and column is achieved by requiring that the column and plate rotations be equal.

This paper describes the modeling procedures for the plate with internal and elastic edge supports as shown in Fig. 1 along with the derivation of the boundary and compatibility conditions. Subsequently, general solutions of the governing differential equations are derived and the eigenvalue equations are presented and solved. In order to verify the accuracy of the present analysis, the solutions are compared with previous research and it is shown that there is good agreement with previous results. Finally, a numerical example is presented along with a discussion of the eigenvalues and corresponding mode shapes obtained from the analyses.

2. Governing differential equation and modeling procedure

2.1. Governing differential equation

The displacements of the plate u, v and w along the x, y and z direction, respectively, are expressed by the three quantities ψ_x, ψ_y and w which describe the transverse displacement of the

plate median surface and the rotations of the cross-section. These fundamental quantities w, ψ_x and ψ_y for the free vibration of the plate can be written as the product of the displacement functions $W(x,y)$, $\Psi_x(x,y)$ and $\Psi_y(x,y)$ and the time-varying function $(A\cos\omega t + B\sin\omega t)$. In this form, the displacements of the plate are

$$u(x,y,z,t) = z\Psi_x(x,y)(A\cos\omega t + B\sin\omega t),$$

$$v(x,y,z,t) = z\Psi_y(x,y)(A\cos\omega t + B\sin\omega t),$$

$$w(x,y,z,t) = W(x,y)(A\cos\omega t + B\sin\omega t), \tag{1}$$

where A and B are unknown constants, and ω is the radian natural frequency of the plate.

Substituting Eq. (1) into the kinetic equations, derived from equations of equilibrium, gives the governing differential equations of the Mindlin plate theory which considers the effects of transverse shear deformation and rotary inertia. For the case where the distributed load $q_z(x,y,t)$ is acting in the vertical direction, the three governing differential equations as presented by Mindlin [10] can be written as

$$\frac{D}{2}\left\{(1-\nu)\left(\frac{\partial^2}{\partial x^2}+\frac{\partial^2}{\partial y^2}\right)\Psi_x + (1+\nu)\frac{\partial}{\partial x}\left(\frac{\partial\Psi_x}{\partial x}+\frac{\partial\Psi_y}{\partial y}\right)\right\} - \kappa Gh\left(\frac{\partial W}{\partial x}+\Psi_x\right) + \frac{\omega^2\rho h^3}{12}\Psi_x = 0,$$

$$\frac{D}{2}\left\{(1-\nu)\left(\frac{\partial^2}{\partial x^2}+\frac{\partial^2}{\partial y^2}\right)\Psi_y + (1+\nu)\frac{\partial}{\partial y}\left(\frac{\partial\Psi_x}{\partial x}+\frac{\partial\Psi_y}{\partial y}\right)\right\} - \kappa Gh\left(\frac{\partial W}{\partial y}+\Psi_y\right) + \frac{\omega^2\rho h^3}{12}\Psi_y = 0,$$

$$\kappa Gh\left\{\left(\frac{\partial^2}{\partial x^2}+\frac{\partial^2}{\partial y^2}\right)W + \frac{\partial\Psi_x}{\partial x}+\frac{\partial\Psi_y}{\partial y}\right\} + \omega^2\rho h W + q_z = 0 \tag{2}$$

in which D is the flexural rigidity of plate, G is the shear modulus, ρ is the density, ν is the Poisson ratio, h is the plate thickness, κ is the shear correction factor, and q_z is the uniform load. These equations do not have the time-varying function as they cancel from both sides of the expressions.

The associated shear forces, bending moments and torsional moments can be written as [10],

$$Q_x = \kappa Gh\left(\frac{\partial W}{\partial x}+\Psi_x\right), \quad Q_y = \kappa Gh\left(\frac{\partial W}{\partial y}+\Psi_y\right),$$

$$M_x = D\left(\frac{\partial\Psi_x}{\partial x}+\nu\frac{\partial\Psi_y}{\partial y}\right), \quad M_y = D\left(\frac{\partial\Psi_y}{\partial y}+\nu\frac{\partial\Psi_x}{\partial x}\right),$$

$$M_{xy} = \frac{1-\nu}{2}D\left(\frac{\partial\Psi_x}{\partial y}+\frac{\partial\Psi_y}{\partial x}\right). \tag{3}$$

2.2. Boundary conditions

The coordinate system of the rectangular plate is set up as shown in Fig. 2(a). For convenience, a plate size of $2a$ in length by $2b$ in width is converted to dimensionless form, shown in Fig. 2(b),

via the transformations $\xi = x/a$ and $\eta = y/b$. In the dimensionless coordinate system, the boundary conditions of the lateral, rotational and torsional elastic edge supports can be written as Eq. (4) by introducing lateral stiffness K_{L1}–K_{L4}, the rotational stiffness K_{R1}–K_{R4} and the torsional stiffness K_{T1}–K_{T4}. The subscripts 1–4 are utilized to indicate the various plate edges as shown in Fig. 1.

$$Q_x(\pm 1,\eta) + K_{L1,2}W(\pm 1,\eta) = 0, \quad Q_y(\xi,\pm 1) + K_{L3,4}W(\xi,\pm 1) = 0,$$

$$M_x(\pm 1,\eta) + K_{R1,2}\Psi_x(\pm 1,\eta) = 0, \quad M_y(\xi,\pm 1) + K_{R3,4}\Psi_y(\xi,\pm 1) = 0,$$

$$M_{xy}(\pm 1,\eta) + K_{T1,2}\Psi_y(\pm 1,\eta) = 0, \quad M_{xy}(\xi,\pm 1) + K_{T3,4}\Psi_x(\xi,\pm 1) = 0, \tag{4}$$

where

$$K_{L1-4} = \frac{ak_{L1-4}}{\kappa Gh}, \quad K_{R1-4} = \frac{ak_{R1-4}}{D}, \quad K_{T1-4} = \frac{2ak_{T1-4}}{(1-\nu)D}$$

in which k_{L1}–k_{L4} are basic lateral spring stiffness along the plate edges, k_{R1}–k_{R4} are basic rotational spring stiffness and k_{T1}–k_{T4} are basic torsional spring stiffness. The stiffnesses along opposite edges should be equal for symmetry, that is, $K_{L1} = K_{L2}$, $K_{L3} = K_{L4}$, $K_{R1} = K_{R2}$, $K_{R3} = K_{R4}$ and $K_{T1} = K_{T2}$, $K_{T3} = K_{T4}$.

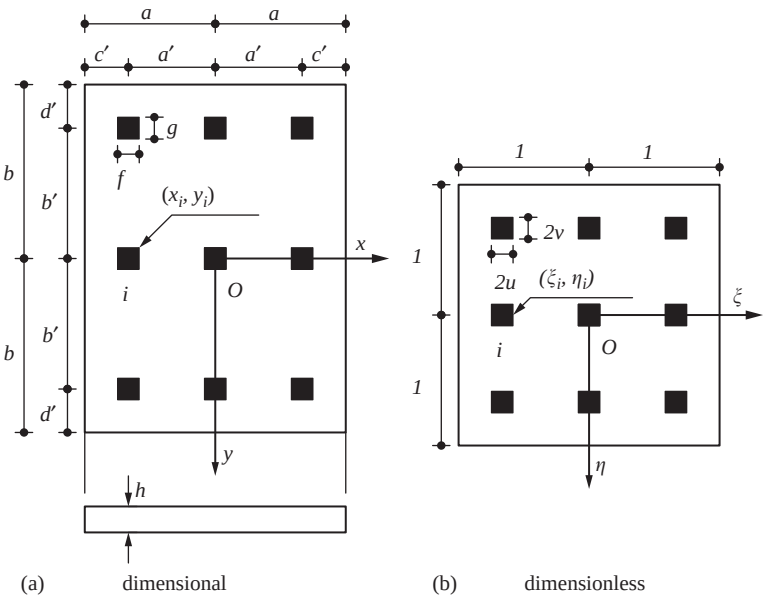

Fig. 2. Coordinate system.

2.3. Compatibility condition of the plate and column

The support condition of the column is taken as either pinned or fixed as shown in Fig. 3. The moment–rotation relationship of the column, at the point of connection between the column and plate, is derived using the Timoshenko beam theory to account for the effect of shear deformation. The relationship between the rotation of column, ${}_c\Psi_{x(y)}$, and the bending moment in the column, ${}_iM_{x(y)}$, (where the subscript i indicates column number) for each support condition are expressed, respectively, as

$$\text{(i) } \textit{Pin support}\text{: } {}_c\Psi_{x(y)} = \frac{l}{EI}\left(\frac{1+\varphi_1}{4+\varphi_1}\right){}_iM_{x(y)},$$

$$\text{(ii) } \textit{Fixed support}\text{: } {}_c\Psi_{x(y)} = \frac{l}{EI}\left(\frac{4+\varphi_1}{12}\right){}_iM_{x(y)}, \tag{5}$$

where

$$\varphi_1 = \frac{12EI}{\kappa GAl^2}$$

in which E is the modulus of elasticity, I is the second moment of area, A is the area of column, and l is the length of column.

The compatibility condition between the column and plate is provided by the assumption that the columns are inextensible and the rotation of the column, ${}_c\Psi_{x(y)}$, with respect to the $x(y)$ direction is equal to the rotation of the plate, ${}_s\Psi_{x(y)}$, at the connection point. These conditions are expressed as follows. It should be noted that the analysis presented here is for the case where the columns are symmetrically distributed.

$${}_s\Psi_x(\xi_i,\eta_i) = {}_c\Psi_x(\xi_i,\eta_i), \quad {}_s\Psi_y(\xi_i,\eta_i) = {}_c\Psi_y(\xi_i,\eta_i), \quad W(\xi_i,\eta_i) = 0. \tag{6}$$

2.4. Assumption of mode type

For the coordinate system shown in Fig. 2, the four mode shapes shown in Fig. 4 can be assumed. The first mode is a symmetric–symmetric mode with respect to the x- and y-axis (denoted SS Mode), the second mode is a symmetric–antisymmetric mode (SA Mode), the third an antisymmetric–symmetric mode (AS Mode), and the fourth an antisymmetric–antisymmetric mode (AA Mode). Corresponding to the mode type, the function is an odd or even function and

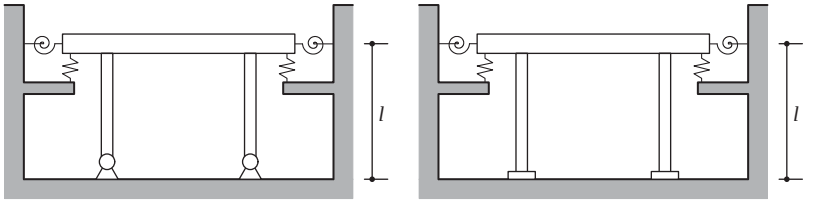

Fig. 3. Schematic showing the different column fixities.

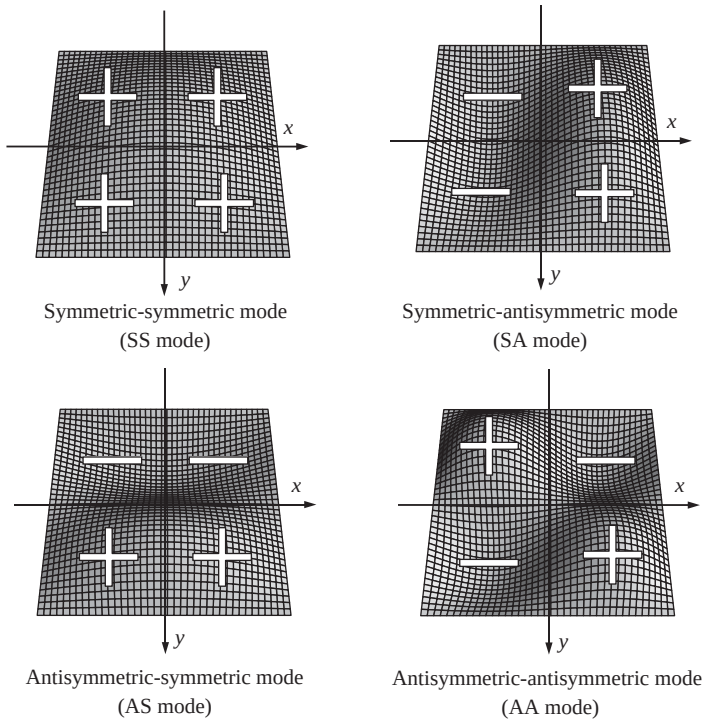

Fig. 4. The four mode shapes considered.

for this reason, it is necessary for the mode type to be assumed prior to deriving the interactive column forces and the general solutions of the governing differential equations. The Lévy-type solution for each mode types is

$$
\begin{aligned}
&SS\ Mode\text{: } W(\xi,\eta) = \sum_{m=1}^{\infty} Y_m(\eta)\cos m\pi\xi + \sum_{n=1}^{\infty} X_n(\xi)\cos n\pi\eta,\\
&SA\ Mode\text{: } W(\xi,\eta) = \sum_{m=1}^{\infty} Y_m(\eta)\sin\frac{(2m-1)\pi}{2}\xi + \sum_{n=1}^{\infty} X_n(\xi)\cos n\pi\eta,\\
&AS\ Mode\text{: } W(\xi,\eta) = \sum_{m=1}^{\infty} Y_m(\eta)\cos m\pi\xi + \sum_{n=1}^{\infty} X_n(\xi)\sin\frac{(2n-1)\pi}{2}\eta,\\
&AA\ Mode\text{: } W(\xi,\eta) = \sum_{m=1}^{\infty} Y_m(\eta)\sin\frac{(2m-1)\pi}{2}\xi + \sum_{n=1}^{\infty} X_n(\xi)\sin\frac{(2n-1)\pi}{2}\eta.
\end{aligned}
\tag{7}
$$

2.5. Interactive forces between column and plate

The interactive forces between the column and plate can be represented by the partial vertical force (acting on the whole cross-section of the column), and a distributed force-couple that results

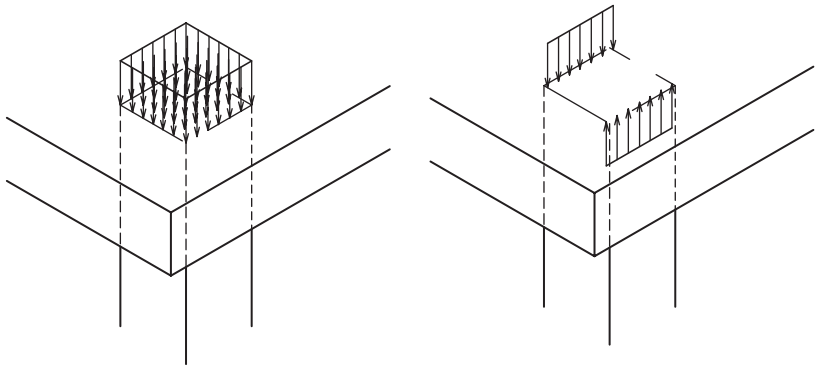

Fig. 5. The interactive forces at the connection between the column and plate.

in an equivalent bending moment, as shown in Fig. 5. The forces are varied in the same phase as the plate vibration and therefore they are expressed in the same manner as the fundamental quantities (w, ψ_x and ψ_y), namely

$$
{}_tP(\xi,\eta,t) = \sum_{i=1}^{N} {}_iP(\xi,\eta)(A\cos\omega t + B\sin\omega t),
$$

$$
{}_tM_x(\xi,\eta,t) = \sum_{i=1}^{N} {}_iM_x(\xi,\eta)(A\cos\omega t + B\sin\omega t),
$$

$$
{}_tM_y(\xi,\eta,t) = \sum_{i=1}^{N} {}_iM_y(\xi,\eta)(A\cos\omega t + B\sin\omega t), \tag{8}
$$

where N is the total number of columns, ${}_tP(\xi,\eta,t)$ is the total vertical force over all columns, and ${}_iP(\xi,\eta)$ is the partial vertical force on the ith column; ${}_tM_x(\xi,\eta,t)$ and ${}_tM_y(\xi,\eta,t)$ are the total bending moments over all columns in the x and y directions, respectively, and ${}_iM_x(\xi,\eta)$ and ${}_iM_y(\xi,\eta)$ are the bending moments at the ith column. Substituting these expressions as the distributed load $q_z(x,y,t)$ in the kinetic equations, one obtains the governing differential equations. The partial vertical force and distributed force-couple given by Dirac's function are expressed by a Fourier series expansion. The loading is dependent on the particular mode as indicated in Section 2.4. For the case of the SS Mode, these forces are

$$
{}_iP(\xi,\eta) = \frac{4\cdot {}_iP_{mn}}{a^2\phi}\sum_{m=1}^{\infty}\sum_{n=1}^{\infty} {}_iC_p\cos\mu_m\xi\cos\mu_n\eta, \tag{9}
$$

$$
{}_iM_x(\xi,\eta) = \frac{2\cdot {}_iM_{xmn}}{a^3\phi}\sum_{m=1}^{\infty}\sum_{n=1}^{\infty} {}_iC_{Mx}\cos\mu_m\xi\cos\mu_n\eta, \tag{10}
$$

$$ {}_iM_y(\xi,\eta) = \frac{2\cdot {}_iM_{ymn}}{a^3\phi^2}\sum_{m=1}^{\infty}\sum_{n=1}^{\infty} {}_iC_{My}\cos\mu_m\xi\cos\mu_n\eta, \tag{11} $$

where

$$ \phi=\frac{b}{a},\ \mu_m=m\pi,\ \mu_n=n\pi,\ m,n=1,2,3,\ldots $$

$$ {}_iC_p = \left(\frac{\cos\mu_m\xi_i\sin\mu_m u}{\mu_m u}\right)\left(\frac{\cos\mu_n\eta_i\sin\mu_n v}{\mu_n v}\right), $$

$$ {}_iC_{Mx} = \left(\frac{\mu_m\sin\mu_m\xi_i\sin\mu_m u}{\mu_m u}\right)\left(\frac{\cos\mu_n\eta_i\sin\mu_n v}{\mu_n v}\right), $$

$$ {}_iC_{My} = \left(\frac{\cos\mu_m\xi_i\sin\mu_m u}{\mu_m u}\right)\left(\frac{\mu_n\sin\mu_n\eta_i\sin\mu_n v}{\mu_n v}\right) $$

in which ϕ is the plate aspect ratio; ${}_iP_{mn}$, ${}_iM_{xmn}$ and ${}_iM_{ymn}$ are unknown constants; and u and v are the half-width of the column section in the x and y directions, respectively. It should be noted that these forces are halved when the column position is on the x- and y-axis of coordinates system. The loading for the other modes (the SA, AS, or AA Mode) is obtained in a similar fashion by replacing the trigonometric function as indicated in Section 2.4.

3. General solution and eigenvalue equation

In this paper, the procedures for the derivation of the general solution and eigenvalue equation are introduced for the SS Mode only. The same procedure can be applied to the other modes by replacing the trigonometric functions appropriately.

3.1. Inhomogeneous solution

In case of the SS Mode, the inhomogeneous solutions of the transverse displacement, ${}_nW(\xi,\eta)$, and the rotation, ${}_n\Psi_x(\xi,\eta)$ and ${}_n\Psi_y(\xi,\eta)$, can be assumed to be of the following form:

$$ {}_nW(\xi,\eta) = \sum_{m=1}^{\infty}\sum_{n=1}^{\infty} W_{mn}\cos\mu_m\xi\cos\mu_n\eta, $$

$$ {}_n\Psi_x(\xi,\eta) = \sum_{m=1}^{\infty}\sum_{n=1}^{\infty} \Psi_{xmn}\sin\mu_m\xi\cos\mu_n\eta, $$

$$ {}_n\Psi_y(\xi,\eta) = \sum_{m=1}^{\infty}\sum_{n=1}^{\infty} \Psi_{ymn}\cos\mu_m\xi\sin\mu_n\eta, \tag{12} $$

where W_{mn}, Ψ_{xmn} and Ψ_{ymn} are unknown constants.

By substituting the above displacements and the interactive partial vertical force given by Eq. (9) into governing differential equations, the unknown constants are determined and each inhomogeneous solution for the case of the partial vertical force are obtained and given by

$$
{}_{np}W(\xi,\eta)=\frac{4a^2\cdot{}_iP_{mn}}{\phi D}\sum_{m=1}^{\infty}\sum_{n=1}^{\infty}{}_iC_p\frac{{}_nC_w}{{}_nC_{\mathrm{deno}}}\cos\mu_m\xi\cos\mu_n\eta,
$$

$$
{}_{np}\Psi_x(\xi,\eta)=\frac{4a\cdot{}_iP_{mn}}{\phi D}\sum_{m=1}^{\infty}\sum_{n=1}^{\infty}{}_iC_p\frac{\mu_m}{{}_nC_{\mathrm{deno}}}\sin\mu_m\xi\cos\mu_n\eta,
$$

$$
{}_{np}\Psi_y(\xi,\eta)=\frac{4a\cdot{}_iP_{mn}}{\phi^2 D}\sum_{m=1}^{\infty}\sum_{n=1}^{\infty}{}_iC_p\frac{\mu_n}{{}_nC_{\mathrm{deno}}}\cos\mu_m\xi\sin\mu_n\eta, \tag{13}
$$

where

$$
{}_nC_w=1+\frac{1}{6(1-\nu)\kappa}\left(\mu_m^2+\frac{\mu_n^2}{\phi^2}\right)\left(\frac{h}{a}\right)^2-\frac{\lambda^2}{72(1-\nu)\kappa}\left(\frac{h}{a}\right)^4,
$$

$$
{}_nC_{\mathrm{deno}}=\left(\mu_m^2+\frac{\mu_n^2}{\phi^2}-\Omega_1\right)\left(\mu_m^2+\frac{\mu_n^2}{\phi^2}-\Omega_2\right),
$$

$$
\Omega_{1,2}=\frac{\lambda^2\{2+(1-\nu)\kappa\}}{24(1-\nu)\kappa}\left(\frac{h}{a}\right)^2\pm\sqrt{\frac{\lambda^4\{2-(1-\nu)\kappa\}^2}{24^2(1-\nu)^2\kappa^2}\left(\frac{h}{a}\right)^4+\lambda^2}\quad(\Omega_1>\Omega_2),
$$

$$
\lambda=\omega a^2\sqrt{\frac{\rho h}{D}}.
$$

For the case of the interactive bending moment, ${}_iM_x(\xi,\eta)$, the inhomogeneous solutions are obtained in the same manner and are given by

$$
{}_{nx}W(\xi,\eta)=\frac{2a\cdot{}_iM_{xmn}}{\phi D}\sum_{m=1}^{\infty}\sum_{n=1}^{\infty}{}_iC_x\frac{{}_nC_w}{{}_nC_{\mathrm{deno}}}\cos\mu_m\xi\cos\mu_n\eta,
$$

$$
{}_{nx}\Psi_x(\xi,\eta)=\frac{2\cdot{}_iM_{xmn}}{\phi D}\sum_{m=1}^{\infty}\sum_{n=1}^{\infty}{}_iC_x\frac{\mu_m}{{}_nC_{\mathrm{deno}}}\sin\mu_m\xi\cos\mu_n\eta,
$$

$$
{}_{nx}\Psi_y(\xi,\eta)=\frac{2\cdot{}_iM_{xmn}}{\phi^2 D}\sum_{m=1}^{\infty}\sum_{n=1}^{\infty}{}_iC_x\frac{\mu_n}{{}_nC_{\mathrm{deno}}}\cos\mu_m\xi\sin\mu_n\eta. \tag{14}
$$

Similarly, the inhomogeneous solutions for the bending moment, ${}_iM_y(\xi,\eta)$, are

$$
{}_{ny}W(\xi,\eta)=\frac{2a\cdot{}_iM_{ymn}}{\phi^2 D}\sum_{m=1}^{\infty}\sum_{n=1}^{\infty}{}_iC_y\frac{{}_nC_w}{{}_nC_{\mathrm{deno}}}\cos\mu_m\xi\cos\mu_n\eta,
$$

$$
{}_{ny}\Psi_x(\xi,\eta) = \frac{2\cdot {}_iM_{ymn}}{\phi^2 D}\sum_{m=1}^{\infty}\sum_{n=1}^{\infty} {}_iC_y \frac{\mu_m}{{}_nC_{\text{deno}}}\sin\mu_m\xi\cos\mu_n\eta,
$$

$$
{}_{ny}\Psi_y(\xi,\eta) = \frac{2\cdot {}_iM_{ymn}}{\phi^3 D}\sum_{m=1}^{\infty}\sum_{n=1}^{\infty} {}_iC_y \frac{\mu_n}{{}_nC_{\text{deno}}}\cos\mu_m\xi\sin\mu_n\eta. \tag{15}
$$

The inhomogeneous solutions for the shear forces, the bending moments and the torsional moments can be derived by substituting the above displacements into Eq. (3).

3.2. Homogeneous solution

In the absence of distributed load, the governing differential equations are transformed to a simplified form through the use of Helmholtz theorem as presented by Mindlin [10], and given by

$$
\left(\frac{\partial^2}{\partial x^2}+\frac{\partial^2}{\partial y^2}+\delta_1^2\right)W_1 = 0,
$$

$$
\left(\frac{\partial^2}{\partial x^2}+\frac{\partial^2}{\partial y^2}+\delta_2^2\right)W_2 = 0,
$$

$$
\left(\frac{\partial^2}{\partial x^2}+\frac{\partial^2}{\partial y^2}+\delta_3^2\right)H = 0 \tag{16}
$$

and expressed in dimensionless form,

$$
\frac{\partial^2 W_1}{\partial\xi^2}+\frac{1}{\phi^2}\frac{\partial^2 W_1}{\partial\eta^2}+\Omega_1 W_1 = 0,
$$

$$
\frac{\partial^2 W_2}{\partial\xi^2}+\frac{1}{\phi^2}\frac{\partial^2 W_2}{\partial\eta^2}+\Omega_2 W_2 = 0,
$$

$$
\frac{\partial^2 H}{\partial\xi^2}+\frac{1}{\phi^2}\frac{\partial^2 H}{\partial\eta^2}+\Omega_3 H = 0, \tag{17}
$$

where

$$
W = W_1 + W_2,
$$

$$
\Psi_x = (s_1-1)\frac{1}{a}\frac{\partial W_1}{\partial\xi}+(s_2-1)\frac{1}{a}\frac{\partial W_2}{\partial\xi}+\frac{1}{a\phi}\frac{\partial H}{\partial\eta},
$$

$$
\Psi_y = (s_1-1)\frac{1}{a\phi}\frac{\partial W_1}{\partial\eta}+(s_2-1)\frac{1}{a\phi}\frac{\partial W_2}{\partial\eta}-\frac{1}{a}\frac{\partial H}{\partial\xi}, \tag{18}
$$

in which

$$\delta_1^2 = \frac{\Omega_1}{a^2}, \quad \delta_2^2 = \frac{\Omega_2}{a^2}, \quad \delta_3^2 = \frac{\Omega_3}{a^2},$$

$$\Omega_3 = \frac{\lambda^2}{6(1-\nu)}\left(\frac{h}{a}\right)^2 - 12\kappa\left(\frac{a}{h}\right)^2,$$

$$s_1 = \frac{2\Omega_2}{(1-\nu)\Omega_3} - 1, \quad s_2 = \frac{2\Omega_1}{(1-\nu)\Omega_3} - 1, \tag{19}$$

where H is the potential. In case of the SS Mode, the homogeneous solutions of the transverse displacement function, $W_{1,2}(\xi,\eta)$, and the potential, $H(\xi,\eta)$, can be expressed by the following equations with the unknown functions ${}_hX_{n1,2}(\xi)$, ${}_hY_{m1,2}(\eta)$ and ${}_hH_n(\xi)$, ${}_hH_m(\eta)$.

$$W_{1,2}(\xi,\eta) = \sum_{m=1}^{\infty} {}_hY_{m1,2}(\eta)\cos\mu_m\xi + \sum_{n=1}^{\infty} {}_hX_{n1,2}(\xi)\cos\mu_n\eta,$$

$$H(\xi,\eta) = \sum_{m=1}^{\infty} {}_hH_m(\eta)\sin\mu_m\xi + \sum_{n=1}^{\infty} {}_hH_n(\xi)\sin\mu_n\eta. \tag{20}$$

Substituting Eq. (20) into the differential equations, given by Eq. (17), one obtains homogeneous, second-order, ordinary differential equations. The ordinary differential equations are solved by assuming appropriate functions consistent with the assumption of the mode type, that is, the symmetric mode type is applied to even functions, while the antisymmetric mode is applied to the odd functions. The homogeneous solutions are obtained by substituting solutions of the ordinary differential equations into Eq. (18). The homogeneous solutions have the following six possible cases with respect to both m [Case(M-1)–Case(M-6)] and n [Case(N-1)–Case(N-6)].

$$\begin{aligned}
&\textit{Case}(\text{M-1}):\ \alpha_m<\beta_m<0 \quad \text{and } \gamma_m<0,\\
&\textit{Case}(\text{M-2}):\ \alpha_m<\beta_m<0 \quad \text{and } \gamma_m>0,\\
&\textit{Case}(\text{M-3}):\ \alpha_m<0<\beta_m \quad \text{and } \gamma_m<0,\\
&\textit{Case}(\text{M-4}):\ \alpha_m<0<\beta_m \quad \text{and } \gamma_m>0,\\
&\textit{Case}(\text{M-5}):\ 0<\alpha_m<\beta_m \quad \text{and } \gamma_m<0,\\
&\textit{Case}(\text{M-6}):\ 0<\alpha_m<\beta_m \quad \text{and } \gamma_m>0,
\end{aligned}$$

$$\begin{aligned}
&\textit{Case}(\text{N-1}):\ \alpha_n<\beta_n<0 \quad \text{and } \gamma_n<0,\\
&\textit{Case}(\text{N-2}):\ \alpha_n<\beta_n<0 \quad \text{and } \gamma_n>0,\\
&\textit{Case}(\text{N-3}):\ \alpha_n<0<\beta_n \quad \text{and } \gamma_n<0,\\
&\textit{Case}(\text{N-4}):\ \alpha_n<0<\beta_n \quad \text{and } \gamma_n>0,\\
&\textit{Case}(\text{N-5}):\ 0<\alpha_n<\beta_n \quad \text{and } \gamma_n<0,\\
&\textit{Case}(\text{N-6}):\ 0<\alpha_n<\beta_n \quad \text{and } \gamma_n>0,
\end{aligned}$$

where

$$\alpha_m^2 = |(\mu_m^2 - \Omega_1)\phi^2|, \quad \beta_m^2 = |(\mu_m^2 - \Omega_2)\phi^2|, \quad \gamma_m^2 = |(\mu_m^2 - \Omega_3)\phi^2|,$$

$$\alpha_n^2 = |\mu_n^2/\phi^2 - \Omega_1|, \quad \beta_n^2 = |\mu_n^2/\phi^2 - \Omega_2|, \quad \gamma_n^2 = |\mu_n^2/\phi^2 - \Omega_3|.$$

In the Case(M-1) and Case(N-6) of the SS Mode, for example, the homogeneous solutions of the transverse displacement, ${}_h W(\xi,\eta)$, and the rotation, ${}_h\Psi_x(\xi,\eta)$ and ${}_h\Psi_y(\xi,\eta)$, are

$$\begin{aligned} {}_h W(\xi,\eta) = {} & \frac{a^2}{D}\sum_{m=1}^{\infty}\left(Y_{m1}\frac{\cos\alpha_m\eta}{\sin\alpha_m} + Y_{m2}\frac{\cos\beta_m\eta}{\sin\beta_m}\right)\cos\mu_m\xi \\ & + \frac{a^2}{D}\sum_{n=1}^{\infty}\left(X_{n1}\frac{\cosh\alpha_n\xi}{\sinh\alpha_n} + X_{n2}\frac{\cosh\beta_n\xi}{\sinh\beta_n}\right)\cos\mu_n\eta, \end{aligned} \tag{21}$$

$$\begin{aligned} {}_h\Psi_x(\xi,\eta) = {} & \frac{a}{D}\sum_{m=1}^{\infty}\left(Y_{m1}\mu_m(s_1-1)\frac{-\cos\alpha_m\eta}{\sin\alpha_m}\right. \\ & \left. + Y_{m2}\mu_m(s_2-1)\frac{-\cos\beta_m\eta}{\sin\beta_m} + Y_{m3}\frac{\gamma_m}{\phi}\frac{\cos\gamma_m\eta}{\sin\gamma_m}\right)\sin\mu_m\xi \\ & + \frac{a}{D}\sum_{n=1}^{\infty}\left(X_{n1}\alpha_n(s_1-1)\frac{\sinh\alpha_n\xi}{\sinh\alpha_n}\right. \\ & \left. + X_{n2}\beta_n(s_2-1)\frac{\sinh\beta_n\xi}{\sinh\beta_n} + X_{n3}\frac{\mu_n}{\phi}\frac{\sinh\gamma_n\xi}{\sinh\gamma_n}\right)\cos\mu_n\eta, \end{aligned} \tag{22}$$

$$\begin{aligned} {}_h\Psi_y(\xi,\eta) = {} & \frac{a}{\phi D}\sum_{m=1}^{\infty}\left(Y_{m1}\alpha_m(s_1-1)\frac{-\sin\alpha_m\eta}{\sin\alpha_m}\right. \\ & \left. + Y_{m2}\beta_m(s_2-1)\frac{-\sin\beta_m\eta}{\sin\beta_m} + Y_{m3}\mu_m\phi\frac{-\sin\gamma_m\eta}{\sin\gamma_m}\right)\cos\mu_m\xi \\ & + \frac{a}{\phi D}\sum_{n=1}^{\infty}\left(X_{n1}\mu_n(s_1-1)\frac{-\cosh\alpha_n\xi}{\sinh\alpha_n}\right. \\ & \left. + X_{n2}\mu_n(s_2-1)\frac{-\cosh\beta_n\xi}{\sinh\beta_n} + X_{n3}\gamma_n\phi\frac{-\cosh\gamma_n\xi}{\sinh\gamma_n}\right)\sin\mu_n\eta \end{aligned} \tag{23}$$

in which Y_{m1}, Y_{m2}, Y_{m3} and X_{n1}, X_{n2}, X_{n3} are unknown constants.

In the other case, Case(M-1)−Case(M-6) and Case(N-1)−Case(N-6), the homogeneous solutions are obtained by replacing the trigonometric functions as follows; if α_m, α_n, β_m, β_n and γ_m, γ_n are smaller than zero, the normal trigonometric functions are applied to each term containing α_m, α_n, β_m, β_n and γ_m, γ_n, whereas, if these values are larger than zero, the hyperbolic trigonometric functions are applied to each term with respect to m and n.

The homogeneous solutions for the shear forces, bending moments and torsional moments can be derived by substituting the above solutions for the displacement and rotation into Eq. (3).

3.3. Generation of the eigenvalue equation

The general solutions are obtained by adding the inhomogeneous solutions and the homogeneous solutions. The general solutions for displacement W, Ψ_x and Ψ_y are then

$$W(\xi,\eta) = {}_hW(\xi,\eta) + {}_{np}W(\xi,\eta) + {}_{nx}W(\xi,\eta) + {}_{ny}W(\xi,\eta),$$

$$\Psi_x(\xi,\eta) = {}_h\Psi_x(\xi,\eta) + {}_{np}\Psi_x(\xi,\eta) + {}_{nx}\Psi_x(\xi,\eta) + {}_{ny}\Psi_x(\xi,\eta),$$

$$\Psi_y(\xi,\eta) = {}_h\Psi_y(\xi,\eta) + {}_{np}\Psi_y(\xi,\eta) + {}_{nx}\Psi_y(\xi,\eta) + {}_{ny}\Psi_y(\xi,\eta). \tag{24}$$

The general solutions for the shear forces, the bending moments and the torsional moments are obtained in an analogous fashion.

With the general solutions obtained above, nine relational equations including the unknown constants can be derived by substituting the general solutions into the boundary conditions given in Eq. (4) and the compatibility conditions given in Eq. (6). The resulting eigenvalue equation in

Table 1
Comparison study of first four frequency parameters, λ, for square plates with lateral elastic edge supports ($K_R = 0$, $K_T = 0$, $\nu = 0.333$, $\kappa = 0.8601$, $h/a = 0.1$)

Lateral stiffness	References	Mode			
		1	2	3	4
$K_L = 0.005$	Present	0.9062	1.2979	1.2979	3.4649
	Gorman [1]	0.9063	1.2978	1.2978	3.4650
	Zhou [5]	0.9063	1.2979	1.2979	3.5301
$K_L = 0.05$	Present	2.3983	3.9034	3.9034	5.6374
	Gorman [1]	2.3983	3.9025	3.9025	5.6375
	Zhou [5]	2.4052	3.9131	3.9131	5.6612

Table 2
Comparison study of the fundamental frequency parameter, λ, for square plates with lateral and rotational elastic edge supports ($K_L = 1500$, $K_T = 0$, $\nu = 0.3$, $\kappa = 0.85$, $h/a = 0.01$)

References	K_R							
	5.0×10^{-8}	5	12.5	25	50	250	1350	5.0×10^{6}
Present	4.9115	7.1156	7.9408	8.3821	8.6581	8.9153	8.9725	8.9857
Gorman [1]	4.9000	7.1150	7.9400	8.3825	8.6575	8.9150	8.9725	8.9850
Saha et al. [4]	4.8575	6.8775	7.6125	8.0000	8.2400	8.4600	8.5100	8.5200

matrix form is then

$$\begin{bmatrix} K_{11} & K_{12} & K_{13} & K_{14} & K_{15} & K_{16} & K_{17} & K_{18} & K_{19} \\ K_{21} & K_{22} & K_{23} & K_{24} & K_{25} & K_{26} & K_{27} & K_{28} & K_{29} \\ K_{31} & K_{32} & K_{33} & K_{34} & K_{35} & K_{36} & K_{37} & K_{38} & K_{39} \\ K_{41} & K_{42} & K_{43} & K_{44} & K_{45} & K_{46} & K_{47} & K_{48} & K_{49} \\ K_{51} & K_{52} & K_{53} & K_{54} & K_{55} & K_{56} & K_{57} & K_{58} & K_{59} \\ K_{61} & K_{62} & K_{63} & K_{64} & K_{65} & K_{66} & K_{67} & K_{68} & K_{69} \\ K_{71} & K_{72} & K_{73} & K_{74} & K_{75} & K_{76} & K_{77} & K_{78} & K_{79} \\ K_{81} & K_{82} & K_{83} & K_{84} & K_{85} & K_{86} & K_{87} & K_{88} & K_{89} \\ K_{91} & K_{92} & K_{93} & K_{94} & K_{95} & K_{96} & K_{97} & K_{98} & K_{99} \end{bmatrix} \begin{Bmatrix} Y_{m1} \\ Y_{m2} \\ Y_{m3} \\ X_{n1} \\ X_{n2} \\ X_{n3} \\ {}_iP \\ {}_iM_x \\ {}_iM_y \end{Bmatrix} = 0 \tag{25}$$

Table 3
Comparison study of first six frequency parameters, λ, for square plates with one central internal point support (Liew et al. [8]: $\nu = 0.3$, others: $\nu = 0.333$; $\kappa = \frac{5}{6}$, $h/a = 0.001$); simply supported—$K_L = 10^7$, $K_R = 0$, $K_T = 0$; clamped—$K_L = 10^7$, $K_R = 10^7$, $K_T = 10^7$; free—$K_L = 0$, $K_R = 0$, $K_T = 0$

Boundary condition	Thickness ratio	References	Mode					
			1	2	3	4	5	6
Simply supported			SS	SA(AS)	AA	SS	SS	SA(AS)
	$h/a = 0.200$	Present	6.413	9.180	13.112	15.853	17.686	18.898
		Liew et al. [8]	8.512	9.538	13.790	16.290	—	19.670
			SA(AS)	SS	AA	SS	SA(AS)	SS
	$h/a = 0.001$	Present	12.334	13.153	19.730	24.670	32.064	36.656
		Liew et al. [8]	12.340	13.530	19.740	24.670	32.080	37.710
		Huang and Thambiratnam [9]	12.338	13.188	19.740	—	—	—
		Kim and Dickinson [12]	12.337	13.293	19.739	24.674	32.076	37.050
Clamped			SS	SA(AS)	AA	SS	SS	SA(AS)
	$h/a = 0.200$	Present	8.758	11.333	15.107	17.293	19.253	20.430
		Liew et al. [8]	10.930	11.570	15.540	17.710	—	21.010
			SA(AS)	SS	AA	SS	SA(AS)	SS
	$h/a = 0.001$	Present	18.348	19.644	27.053	32.894	42.248	46.554
		Liew et al. [8]	18.350	20.220	27.050	32.890	41.250	47.800
		Kim and Dickinson [12]	18.349	20.075	27.055	32.895	41.250	47.493
Free			SS	AA	SS	SA(AS)	SS	SA(AS)
	$h/a = 0.200$	Present	1.957	2.857	4.263	6.765	6.800	11.202
		Liew et al. [8]	2.731	2.825	4.350	6.893	8.140	11.310
			SS	AA	SS	SA(AS)	SS	SA(AS)
	$h/a = 0.001$	Present	2.823	3.291	4.806	8.555	11.410	15.232
		Liew et al. [8]	2.831	3.367	4.899	8.700	11.700	15.270
		Raju and Amba-Rao [11]	2.824	3.291	4.805	8.557	11.417	15.233

or in abbreviated form

$$[\boldsymbol{K}]\{\boldsymbol{X}\} = 0 \tag{26}$$

where $[\boldsymbol{K}]$ is the eigenvalue matrix and $\{\boldsymbol{X}\}$ is the eigenvector of unknown constants. With the eigenvalues obtained numerically, using an appropriate method such as the regula falsi method, the corresponding eigenvectors are obtained along with the unknown constants. By applying these constants to the general solution, the mode shapes are obtained.

4. Comparison and convergency studies

4.1. Comparison with other researchers

In order to verify the accuracy of the method, the present solutions are compared to the results of other researchers. As there is no research for the case of simultaneous edge and inner column supports, comparisons are made with previous research reported for the case of elastic edge supports and column supports alone. In the following numerical computations, convergence is achieved by considering 61 terms (as shown in the next section), and the eigenvalue is evaluated by using a value of frequency parameter λ, instead of frequency ω, given by

$$\lambda = \omega a^2 \sqrt{\frac{\rho h}{D}}. \tag{27}$$

Tables 1 and 2 show the frequency parameters, λ, for square plates with uniform elastic edge supports. Table 1 shows a comparison for the case of lateral elastic supports alone ($K_R = 0, K_T = 0$). To be consistent with the values reported in the literature, the Poisson ratio, $v = 0.333$, the shear correction factor, $\kappa = 0.8601$ and the thickness ratio, $h/a = 0.1$. As shown in Table 1, the values presented here agree closely with those reported by Gorman [1] and Zhou [5].

Table 4
Comparison study of first eight frequency parameters, λ, for square plates resting all edges free with four point supports on diagonals (present, Liew et al. [8]: $v = 0.3$, Gorman [7], Raju and Amba-Rao [11]: $v = 0.333$; $\kappa = \frac{5}{6}$, $h/a = 0.001$)

Cantilever ratio	References	Mode							
		1	2	3	4	5	6	7	8
$c'/a' = 2.0$		SS	SA	AS	AA	SS	SA	AS	SS
	Present	3.319	3.382	3.382	4.040	4.899	9.367	9.367	13.312
	Liew et al. [8]	3.327	3.478	3.480	4.217	4.899	9.407	9.408	13.370
	Gorman [7]	3.343	3.384	3.384	—	4.806	9.203	9.203	13.140
	Raju and Amba-Rao [11]	3.343	3.388	3.388	3.975	4.805	9.203	9.203	13.138
$c'/a' = 0.333$		SS	SS	SA	AS	SA	AS	AA	SS
	Present	4.899	5.747	8.067	8.067	11.826	11.826	12.803	13.611
	Liew et al. [8]	4.899	5.756	8.095	8.096	11.960	11.960	13.000	14.010
	Gorman [7]	4.806	5.780	7.943	7.943	11.840	11.840	—	13.620
	Raju and Amba-Rao [11]	4.805	5.780	7.943	7.943	11.845	11.845	12.772	13.642

Table 2 shows the fundamental frequency parameter for the case of both lateral and rotational elastic supports. The value of lateral stiffness K_L is fixed as 1500, whereas, the rotational stiffness K_R is varied in the range of 5.0×10^{-8} to 5.0×10^{6}. For this case, the value of the Poisson ratio, $v = 0.3$, the shear correction factor, $\kappa = 0.85$ and the thickness ratio $h/a = 0.01$ are used. Table 2 shows that there is good agreement between the method presented here and that reported by Gorman [1] and Saha et al. [4].

Tables 3 and 4 show the frequency parameters for square plates with inner point supports and various classical boundary conditions. In the present analysis, the boundary condition for a simply supported plate is realized by setting the lateral stiffness, $K_L = 10^7$, and the rotational and torsional stiffness $K_R = 0, K_T = 0$. In the same manner, the clamped boundary condition is realized by setting $K_L = 10^7, K_R = 10^7, K_T = 10^7$, whereas, for the free boundary $K_L = 0, K_R = 0, K_T = 0$. The shape parameters of plate with columns are set to a cantilever ratio c'/a' and a span a' as shown in Fig. 2, and the column length l is set up to $0.6a'$. Table 3 shows the first six frequency parameters with one central internal point support for the three different boundary conditions considered. For all analyses, the value of the Poisson ratio, $v = 0.333$, except for Liew

Table 5
Convergency study of frequency parameters, λ, with respect to the number of terms included in the Fourier series for three configurations ($v = 0.3$, $\kappa = \frac{5}{6}$)

Condition	Term number	Mode				
		1	2	3	4	5
2×2 column configuration	11	15.1152	33.2943	39.5387	54.5314	64.9449
Mode type SA	21	15.1159	33.2987	39.5422	54.5360	64.9627
$h/a = 0.05$	31	15.1160	33.2988	39.5422	54.5358	64.9620
$c'/a' = 0.10$	41	15.1160	33.2987	39.5422	54.5358	64.9621
$2u, 2v = 0.10$	51	15.1160	33.2990	39.5424	54.5359	64.9629
	61	15.1160	33.2987	39.5422	54.5358	64.9622
	71	15.1160	33.2988	39.5423	54.5358	64.9625
3×3 column configuration	11	22.3381	42.9008	49.8601	68.8245	73.0709
Mode type AA	21	22.3091	42.8993	49.7373	68.7223	73.0712
$h/a = 0.10$	31	22.3097	42.8993	49.7410	68.7256	73.0712
$c'/a' = 0.20$	41	22.3115	42.8994	49.7481	68.7312	73.0714
$2u, 2v = 0.10$	51	22.3119	42.8994	49.7496	68.7323	73.0716
	61	22.3114	42.8994	49.7477	68.7308	73.0715
	71	22.3113	42.8994	49.7471	68.7302	73.0716
4×4 column configuration	11	53.9023	59.4406	59.4440	62.6237	107.9699
Mode type SS	21	53.7146	58.1433	58.1460	61.9823	107.2492
$h/a = 0.01$	31	53.8527	58.6431	58.6447	62.2032	107.6486
$c'/a' = 0.30$	41	53.8632	58.6327	58.6342	62.1979	107.6734
$2u, 2v = 0.20$	51	53.8384	58.5526	58.5544	62.1627	107.5937
	61	53.8435	58.5656	58.5673	62.1683	107.6098
	71	53.8507	58.5922	58.5938	62.1801	107.6323

Table 6
Frequency parameters, λ, for rectangular plate with internal column resting on uniform elastic edge supports ($v = 0.3$, $\kappa = \frac{5}{6}$) 2×2 column configuration, pin support, $\phi = 1.0$, $c'/a' = 0.2$, $K_L = 10.0$, $K_R = 10.0$, $K_T = 10.0$

Mode type	Column area $2u, 2v$	Thickness ratio											
		$h/a = 0.01$				$h/a = 0.05$				$h/a = 0.10$			
		Mode				Mode				Mode			
		1	2	3	4	1	2	3	4	1	2	3	4
SS Mode	0	8.410	29.156	33.074	60.544	8.190	28.044	31.399	55.603	7.742	25.343	27.869	46.448
	0.1	9.020	29.436	34.796	64.538	8.394	28.089	32.131	57.526	7.900	25.351	28.606	48.592
	0.2	9.614	29.760	36.376	67.322	9.079	28.378	33.912	61.153	8.230	25.446	29.488	50.353
	0.3	10.578	30.480	38.596	69.472	10.035	28.939	36.063	63.753	8.874	25.711	30.840	52.284
SA Mode	0	17.609	42.157	50.567	73.504	16.979	39.633	47.259	67.257	15.628	34.435	40.549	55.513
	0.1	18.692	44.177	53.018	77.493	17.378	40.453	48.235	68.225	15.987	35.262	41.528	56.147
	0.2	19.736	45.754	55.936	80.922	18.561	42.361	50.926	71.895	16.567	36.157	42.733	57.423
	0.3	21.380	47.790	60.881	85.872	20.153	44.367	55.142	76.477	17.599	37.449	44.851	59.857
AA Mode	0	28.725	54.475	68.982	98.744	27.127	50.898	62.864	88.144	24.040	43.490	51.770	69.784
	0.1	31.660	56.548	73.105	103.524	28.280	51.244	65.032	90.099	25.169	43.552	54.261	72.288
	0.2	34.640	58.551	76.970	107.734	31.471	53.221	68.940	94.505	26.717	44.192	56.099	73.882
	0.3	39.344	62.406	81.791	112.640	35.886	56.353	73.257	99.205	29.366	45.703	58.410	76.287

Table 7
Frequency parameters, λ, for rectangular plate with internal column resting on uniform elastic edge supports ($v = 0.3$, $\kappa = \frac{5}{6}$) 3×3 column configuration, pin support, $\phi = 1.5$, $c'/a' = 0.2$, $K_L = 10.0$, $K_R = 100.0$, $K_T = 100.0$

Mode type	Column area $2u, 2v$	Thickness ratio											
		$h/a = 0.01$				$h/a = 0.05$				$h/a = 0.10$			
		Mode				Mode				Mode			
		1	2	3	4	1	2	3	4	1	2	3	4
SS Mode	0	13.993	27.840	35.285	46.091	13.661	26.835	34.503	44.666	12.900	24.669	32.533	41.529
	0.1	14.678	29.788	35.894	48.496	13.988	27.789	34.796	45.662	13.287	25.783	32.886	42.494
	0.2	15.363	31.853	36.514	50.710	14.840	30.227	35.540	48.342	13.870	27.396	33.380	44.033
	0.3	16.341	34.900	37.409	53.758	15.856	33.286	36.438	51.427	14.745	29.836	34.108	46.371
SA Mode	0	17.940	28.361	48.502	53.993	17.609	27.793	47.380	52.415	16.879	26.467	44.473	48.641
	0.1	20.168	32.002	51.426	55.458	18.312	28.641	47.997	53.029	17.180	26.820	44.638	49.213
	0.2	21.218	34.839	53.528	56.790	20.293	32.345	50.791	54.597	18.271	28.268	45.634	50.137
	0.3	22.352	38.672	55.680	59.705	21.706	36.598	53.599	56.965	19.856	31.463	47.778	51.569
AA Mode	0	20.334	36.403	54.258	62.776	20.089	35.708	52.851	61.009	19.426	33.929	49.175	56.558
	0.1	20.752	37.629	54.952	64.761	20.185	36.003	53.029	61.473	19.461	34.061	49.260	56.737
	0.2	21.124	38.721	55.480	66.437	20.635	37.321	53.723	63.542	19.652	34.634	49.570	57.605
	0.3	21.701	40.392	56.189	68.949	21.232	39.048	54.488	66.122	20.086	35.879	50.153	59.474

et al. [8], where $v = 0.3$. The shear correction factor, $\kappa = \frac{5}{6}$. The present solution and Liew's solutions consider the effect of shear deformation, and therefore the frequency parameters decrease as the thickness ratio increases. As shown for the case of simply supported and clamped plates, the consideration of shear deformation changes the ordering of the mode types. When the thickness ratio is small, $h/a = 0.001$, the solutions presented here show a good agreement with previous research making use of the thin plate theory. Table 4 shows the frequency parameters for plates with all edges free and four point supports on the diagonals. The value of the Poisson ratio, $v = 0.3$, for the analyses presented here and Liew et al. [8], whereas, $v = 0.333$ for the analysis presented in Gorman [7] and Raju and Amba-Rao [11]. The shear correction factor, $\kappa = \frac{5}{6}$ and the thickness ratio $h/a = 0.001$ are used in order to compare with the values obtained using the thin plate theory. It is seen that the present results agree with the values of Liew et al. [8], Gorman [7] and Raju and Amba-Rao [11].

4.2. Convergency studies

The superposition method can obtain arbitrarily accurate solutions by selecting the number of terms in the Fourier series. In this study, the convergence is examined under three conditions as shown in Table 5. The values of the Poisson ratio, $v = 0.3$, and the shear correction factor, $\kappa = \frac{5}{6}$ are used. This table confirms that the convergence is rapid for each mode under all conditions. For all analyses reported in this paper, the number of terms in the Fourier series is 61.

Table 8
Frequency parameters, λ, for rectangular plate with internal column resting on uniform elastic edge supports ($v = 0.3$, $\kappa = \frac{5}{6}$) 4×4 column configuration, fixed support, $\phi = 1.0$, $c'/a' = 0.3$, $K_L = 10.0$, $K_R = 100.0$, $K_T = 100.0$

Mode type	Column area $2u, 2v$	Thickness ratio											
		$h/a = 0.01$				$h/a = 0.05$				$h/a = 0.10$			
		Mode				Mode				Mode			
		1	2	3	4	1	2	3	4	1	2	3	4
SS Mode	0	38.192	38.637	47.403	55.717	37.629	38.020	45.640	54.938	36.196	36.513	41.371	52.882
	0.1	50.510	51.899	51.998	60.249	41.645	41.956	47.633	56.256	37.339	37.642	43.861	53.289
	0.2	54.107	59.053	59.058	62.888	51.982	54.025	54.062	60.589	43.278	43.496	47.451	55.446
	0.3	58.827	65.694	67.204	67.306	57.180	63.833	64.078	64.506	52.177	53.218	53.290	59.112
SA Mode	0	43.946	46.114	78.144	85.604	42.722	45.284	76.755	82.797	39.607	43.403	73.075	76.024
	0.1	51.438	55.756	91.672	93.526	45.491	48.220	80.567	85.836	41.497	44.348	74.161	79.218
	0.2	56.509	60.989	97.199	103.754	53.124	57.117	93.028	95.417	45.971	48.790	80.005	84.230
	0.3	62.876	66.853	104.089	117.122	60.479	64.378	100.725	110.740	52.878	55.995	91.006	91.916
AA Mode	0	46.248	77.284	86.956	118.181	45.012	75.412	84.481	114.971	42.073	70.886	78.351	106.833
	0.1	53.647	90.111	95.706	129.529	47.570	79.376	87.581	118.045	43.665	72.958	80.582	107.700
	0.2	58.717	99.026	102.353	136.322	55.135	92.118	96.881	128.511	47.827	79.055	85.602	112.190
	0.3	65.047	110.442	111.130	144.337	62.483	105.027	106.674	137.955	54.493	89.527	93.911	120.183

5. Numerical results and discussion

The frequency parameters for the rectangular plate with uniform elastic edge and column supports are tabulated in Tables 6–8. The frequency parameters are presented for each mode type for the thickness ratios, $h/a = 0.01, 0.05$ and 0.10. All analyses are performed with the Poisson ratio, $v = 0.3$, the shear correction factor, $\kappa = \frac{5}{6}$, and the length of column, $l = 0.6a'$. Table 6 presents the results for a square plate supported by 4 pinned columns (in a 2×2 configuration), where the lateral, rotational and torsional stiffnesses are $K_L = 10.0$, $K_R = 10.0$ and $K_T = 10.0$, respectively. In Tables 7 and 8, $K_L = 10.0$, $K_R = 100.0$ and $K_T = 100.0$. Table 7 shows the results for a plate with aspect ratio $\phi = 1.5$, supported by 9 pinned columns (3×3 configuration), and Table 8 presents the results for a square plate supported by 16 fixed-based columns (4×4 configuration).

It is seen that the frequency parameters decrease with increasing thickness ratio. This result is only realized through the use of the Mindlin plate theory as the effect of shear deformation

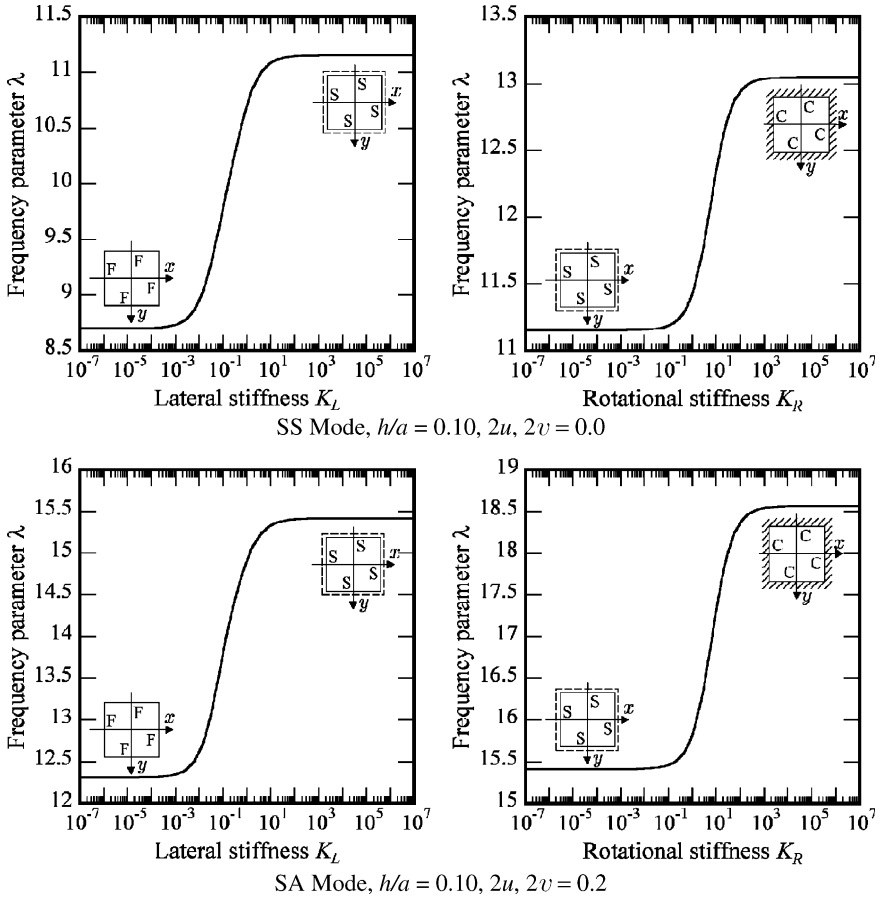

Fig. 6. Eigenvalue variation for increasing values of K_L or K_R (3×3 column configuration, pin support, $\phi = 1.5$, $c'/a' = 0.2$).

increases with increasing plate thickness. For each particular mode type and thickness ratio, the frequency parameters increase with column area, as the restraint of column increases as the cross-sectional area of the column increases. As expected, it is seen that the frequency parameter increases with the number of columns providing restraint.

Figs. 6 and 7 show eigenvalue variations according to increasing lateral and rotational stiffnesses. The conditions of Figs. 6 and 7 correspond to Tables 7 and 8, respectively. The graphs in the left column vary the lateral stiffness while the rotational and torsional stiffness are zero. The figures show the variation in the eigenvalue as the edge supports transition from free to simply supported. Therefore, the lower limit for the lateral stiffness ($K_L = 10^{-7}$) corresponds to the eigenvalue for the free boundary condition, whereas, the upper limit ($K_L = 10^{7}$) corresponds to the eigenvalue for a plate with simply supported edges. In the same manner, the columns on right vary the rational stiffness while fixing the lateral stiffness to $K_L = 10^{7}$ and the torsional stiffness to zero and show the variation in the eigenvalue from simply supported to clamped edges.

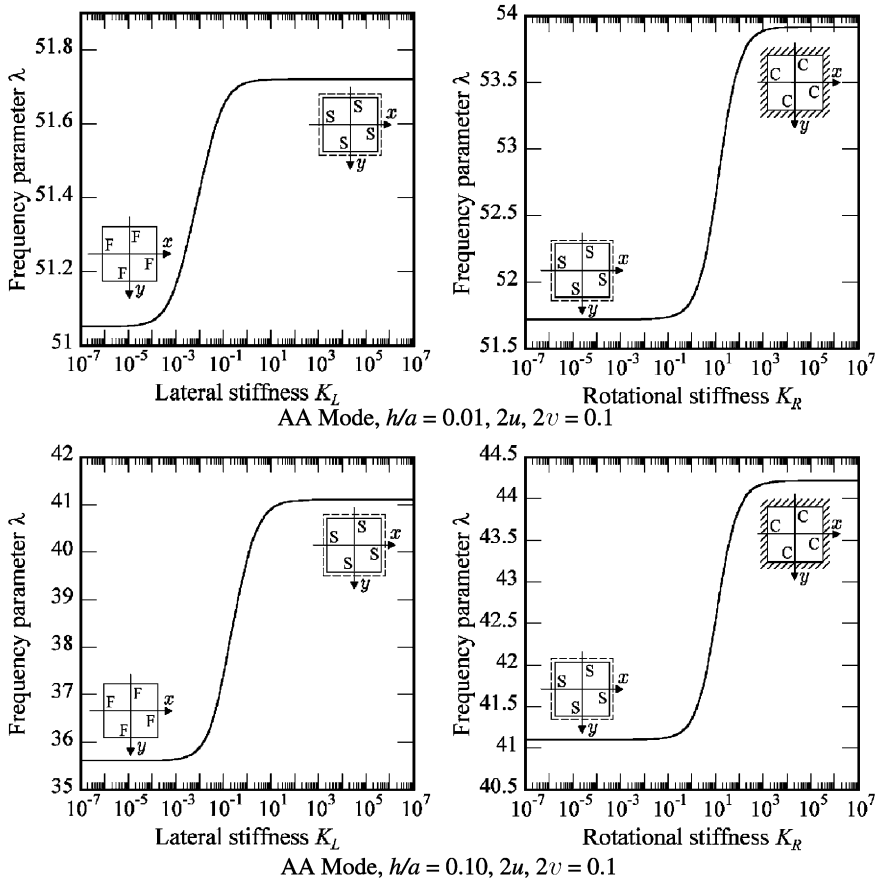

Fig. 7. Eigenvalue variation for increasing values of K_L or K_R (4×4 column configuration, fixed support, $\phi = 1.0$, $c'/a' = 0.3$).

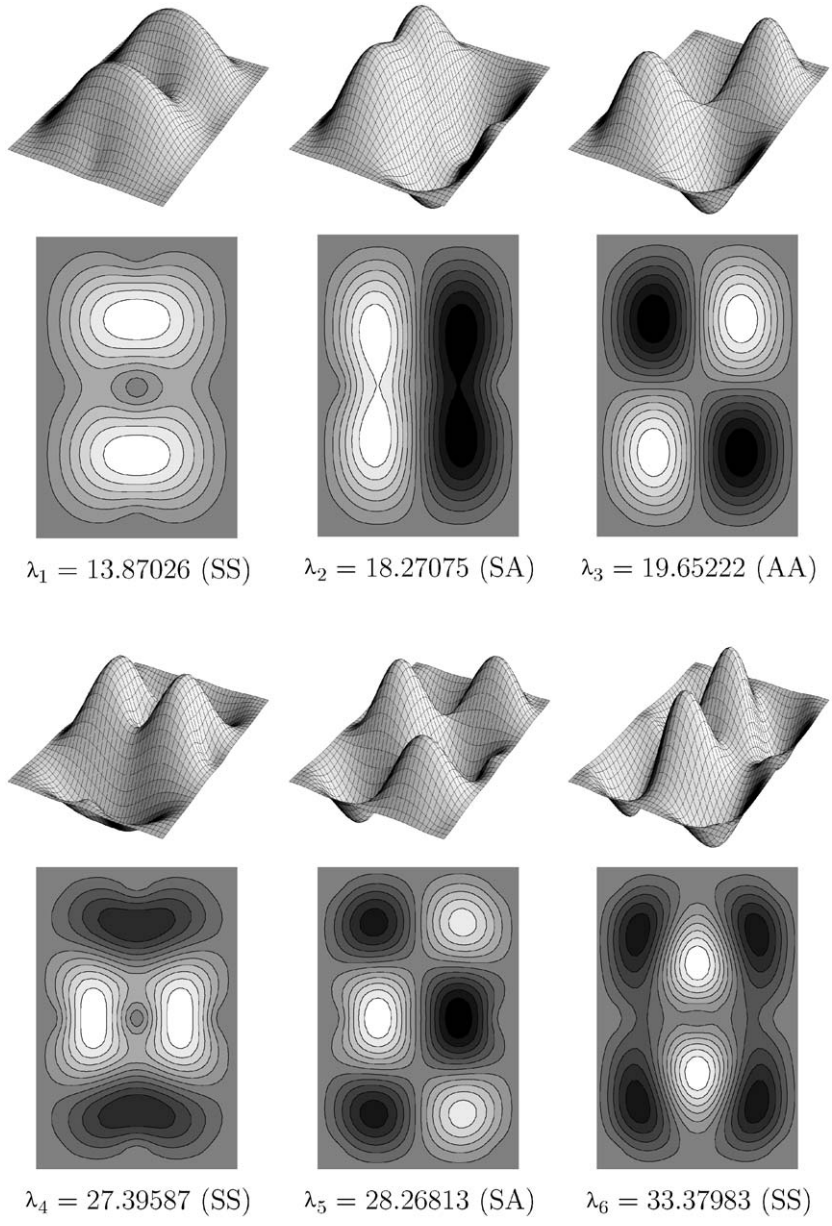

Fig. 8. Mode shape 1 (3×3 column configuration, pin support, $\phi = 1.5$, $c'/a' = 0.2$, $K_L = 10.0$, $K_R = 100.0$, $K_T = 100.0$, $h/a = 0.10$, $2u, 2v = 0.2$).

Figs. 8 and 9 show the first six mode shapes corresponding to the parameters in Table 7 ($h/a = 0.10,\ 2u, 2v = 0.2$) and Table 8 ($h/a = 0.10,\ 2u, 2v = 0.1$), respectively. The modes are shown in order of increasing frequency parameters. The figures show that the mode shapes change considerably for small changes in the frequency parameters.

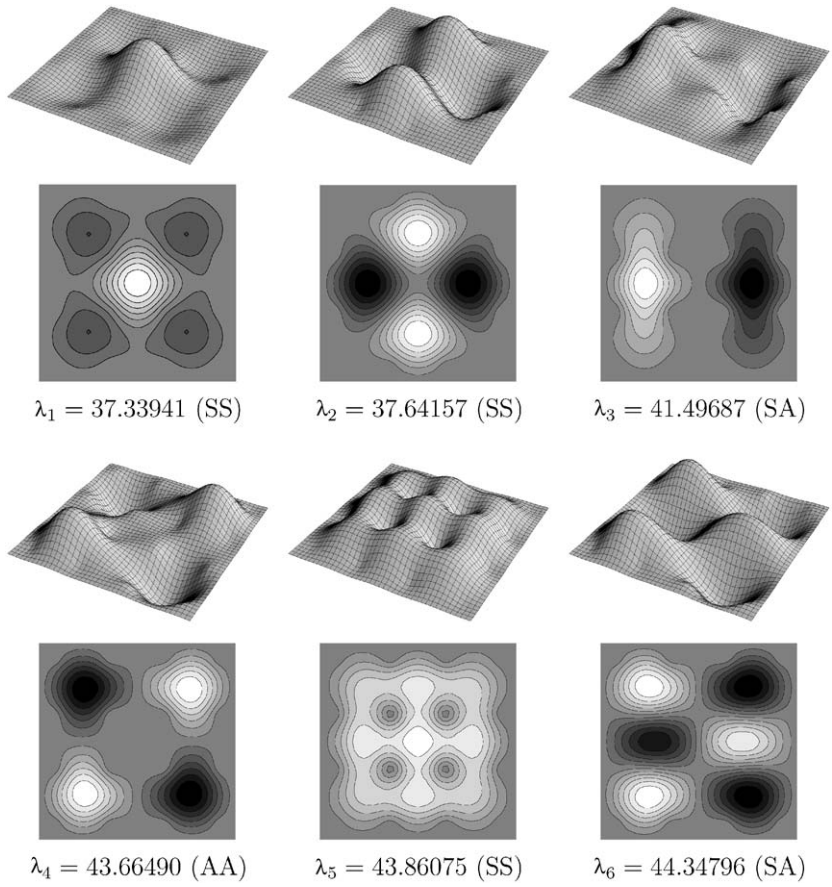

Fig. 9. Mode shape 2 (4×4 column configuration, fixed support, $\phi = 1.0$, $c'/a' = 0.3$, $K_L = 10.0$, $K_R = 100.0$, $K_T = 100.0$, $h/a = 0.10$, $2u, 2v = 0.1$).

6. Conclusions

This paper presents an analytical method for the free vibration analysis of rectangular Mindlin plates with simultaneous lateral, rotational and torsional elastic edge supports and internal column supports, using superposition method. The accuracy of the present analytical method was verified through comparisons with the results from other researchers. The analytical method can be applied for the case of elastic edge supports, classical boundary conditions or mixed boundary conditions, by setting the stiffness to appropriate values. The method accounts for the effect of internal column restraint which increases with the column number and area. Furthermore, as the present analytical method is based on Mindlin plate theory, the effects of transverse shear deformation and rotary inertia are considered. It was shown that the eigenvalues decrease for increasing plate thickness due to the effect of shear deformation. Finally, numerical examples were presented for various conditions for the reference of other researchers.

References

[1] D.J. Gorman, Free vibration analysis of Mindlin plates with uniform elastic edge support by the superposition method, *Journal of Sound and Vibration* 207 (1997) 335–350.
[2] D.J. Gorman, A general solution for the free vibration of rectangular plates with arbitrarily distributed lateral and rotational elastic edge support, *Journal of Sound and Vibration* 174 (1994) 451–459.
[3] Y. Xiang, K.M. Liew, S. Kitipornchai, Vibration analysis of rectangular Mindlin plates resting on elastic edge supports, *Journal of Sound and Vibration* 204 (1997) 1–16.
[4] K.N. Saha, R.C. Kar, P.K. Datta, Free vibration analysis of rectangular Mindlin plates with elastic restraints uniformly distributed along the edges, *Journal of Sound and Vibration* 192 (1996) 885–904.
[5] D. Zhou, Vibrations of Mindlin rectangular plates with elastically restrained edges using static Timoshenko beam functions with the Rayleigh–Ritz method, *Journal of Solids and Structures* 38 (2001) 5565–5580.
[6] D.J. Gorman, Accurate free vibration analysis of point supported Mindlin plates by the superposition method, *Journal of Sound and Vibration* 219 (1999) 265–277.
[7] D.J. Gorman, An analytical solution for the free vibration analysis of rectangular plates resting on symmetrically distributed point supports, *Journal of Sound and Vibration* 79 (1981) 561–574.
[8] K.M. Liew, Y. Xiang, S. Kitipornchai, M.K. Lim, Vibration of Mindlin plates on point supports using constraint functions, *Journal of Engineering Mechanics* 120 (1994) 499–513.
[9] M.-H. Huang, D.P. Thambiratnam, Free vibration analysis of rectangular plates on elastic intermediate supports, *Journal of Sound and Vibration* 240 (2001) 567–580.
[10] R.D. Mindlin, Influence of rotatory inertia and shear on flexural motions of isotropic, elastic plates, *Journal of Applied Mechanics* 18 (1951) 31–38.
[11] I.S. Raju, C.L. Amba-Rao, Free vibrations of a square plate symmetrically supported at four points on the diagonals, *Journal of Sound and Vibration* 90 (1983) 291–297.
[12] C.S. Kim, S.M. Dickinson, The flexural vibration of rectangular plates with point supports, *Journal of Sound and Vibration* 117 (1987) 249–261.